Local structures in ionic liquids probed and characterized by microscopic thermal diffusion monitored with picosecond time-resolved Raman spectroscopy

Kyousuke Yoshida, Koichi Iwata, Yoshio Nishiyama, Yoshifumi Kimura, and Hiro-o Hamaguchi

Citation: The Journal of Chemical Physics **136**, 104504 (2012); doi: 10.1063/1.3691839
View online: http://dx.doi.org/10.1063/1.3691839
View Table of Contents: http://scitation.aip.org/content/aip/journal/jcp/136/10?ver=pdfcov
Published by the AIP Publishing

Local structures in ionic liquids probed and characterized by microscopic thermal diffusion monitored with picosecond time-resolved Raman spectroscopy

Kyousuke Yoshida,[1] Koichi Iwata,[2,a)] Yoshio Nishiyama,[3,b)] Yoshifumi Kimura,[3] and Hiro-o Hamaguchi[1,4,a)]

[1]*Department of Chemistry, School of Science, The University of Tokyo, 7-3-1 Hongo, Bunkyo-ku, Tokyo 113-0033, Japan*
[2]*Department of Chemistry, Faculty of Science, Gakushuin University, Mejiro 1-5-1, Toshima-ku, Tokyo 171-8588, Japan*
[3]*Department of Chemistry, Graduate School of Science, Kyoto University, Kyoto 606-8502, Japan*
[4]*Institute of Molecular Science and Department of Applied Chemistry, National Chiao Tung University, 1001 Ta Hsueh Road, Hsinchu 300, Taiwan*

(Received 8 December 2011; accepted 10 February 2012; published online 8 March 2012)

Vibrational cooling rate of the first excited singlet (S_1) state of *trans*-stilbene and bulk thermal diffusivity are measured for seven room temperature ionic liquids, C_2mimTf_2N, C_4mimTf_2N, C_4mimPF_6, C_5mimTf_2N, C_6mimTf_2N, C_8mimTf_2N, and $bmpyTf_2N$. Vibrational cooling rate measured with picosecond time-resolved Raman spectroscopy reflects solute-solvent and solvent-solvent energy transfer in a microscopic solvent environment. Thermal diffusivity measured with the transient grating method indicates macroscopic heat conduction capability. Vibrational cooling rate of S_1 *trans*-stilbene is known to have a good correlation with bulk thermal diffusivity in ordinary molecular liquids. In the seven ionic liquids studied, however, vibrational cooling rate shows no correlation with thermal diffusivity; the observed rates are similar (0.082 to 0.12 ps^{-1} in the seven ionic liquids and 0.08 to 0.14 ps^{-1} in molecular liquids) despite large differences in thermal diffusivity (5.4–7.5 $\times$ 10^{-8} m^2 s^{-1} in ionic liquids and 8.0–10 $\times$ 10^{-8} m^2 s^{-1} in molecular liquids). This finding is consistent with our working hypothesis that there are local structures characteristically formed in ionic liquids. Vibrational cooling rate is determined by energy transfer among solvent ions in a local structure, while macroscopic thermal diffusion is controlled by heat transfer over boundaries of local structures. By using "local" thermal diffusivity, we are able to simulate the vibrational cooling kinetics observed in ionic liquids with a model assuming thermal diffusion in continuous media. The lower limit of the size of local structure is estimated with vibrational cooling process observed with and without the excess energy. A quantitative discussion with a numerical simulation shows that the diameter of local structure is larger than 10 nm. If we combine this lower limit, 10 nm, with the upper limit, 100 nm, which is estimated from the transparency (no light scattering) of ionic liquids, an order of magnitude estimate of local structure is obtained as 10 nm $< L <$ 100 nm, where L is the length or the diameter of the domain of local structure. © *2012 American Institute of Physics*. [http://dx.doi.org/10.1063/1.3691839]

I. INTRODUCTION

It is gradually being accepted that room temperature of ionic liquids tend to form specific local structures that are not common in ordinary molecular liquids.[1] This tendency is consistent with the fact that ionic liquids are composed solely of ions and that long range Coulombic interaction is dominantly working between ions. Information on these possible local structures in ionic liquids has been collected by Raman spectroscopy,[1] x ray diffraction,[2–5] neutron scattering,[6,7] diffusion measurement,[8,9] acoustic velocity measurement,[10] or molecular dynamics simulation.[11–15] If there are local structures formed in ionic liquids, resultant inhomogeneity is likely to cause discord between microscopic properties determined within a local structure and macroscopic properties measured as a bulk material. In fact, microscopic viscosity determined by the photoisomerization rate of S_1 *trans*-stilbene does not accord with macroscopic shear viscosity in ionic liquids, although these two quantities show clear linear relationship in molecular liquids.[16] This observation was one of the earliest alerts concerning the discord between microscopic and macroscopic properties in ionic liquids.

Thermal diffusion may also be significantly affected by local structure formation. It is controlled by thermal conductivity and heat capacity of a matter, both of which depend on local as well as bulk structures in different fashions. Macroscopic thermal diffusion can be precisely observed by the transient grating (TG) method.[17] In this method, two pulsed laser beams crossing at a sample liquid containing a probe

a)Authors to whom correspondence should be addressed. Electronic addresses: koichi.iwata@gaskushuin.ac.jp and hhama@chem.s.u-tokyo.ac.jp.
b)Present address: Department of Photo-Molecular Science, Institute for Molecular Science, Myodaiji, Okazaki 444-8585, Japan.

dye form a periodic interference pattern. The light energy absorbed by the dye molecules is eventually converted to heat. It increases the temperature of the sample liquid, or changes its refractive index, according to the formed interference pattern of the two laser beams. The periodic pattern of the index functions as a temporarily evolving grating as the generated heat dissipates. It is therefore possible to observe the heat diffusion process by monitoring the time dependence of the probe light intensity diffracted by the grating. Spacing of the interference pattern used by the transient grating method is on the order of laser wavelength or longer. The heat diffusion measured by the transient grating method thus represents thermal diffusion of the sample liquid for a micrometer region or larger. Microscopic energy transfer within the range of a few or a few tens of nanometers can be observed by the vibrational cooling process of the S_1 (the first excited singlet) state of *trans*-stilbene with picosecond time-resolved Raman spectroscopy.[18,19] When *trans*-stilbene is photo-excited with an excess energy, hot S_1 *trans*-stilbene is formed and it starts cooling down immediately. The cooling process, proceeding in approximately 10 ps, is observed with the peak position of the 1570-cm^{-1} Raman band of S_1 *trans*-stilbene. It has been shown by us that the position of the 1570-cm^{-1} band is a linear function of temperature. We use this band as a "picosecond Raman thermometer". The vibrational cooling rate of S_1 *trans*-stilbene thus observed by picosecond time-resolved Raman spectroscopy shows a good correlation with bulk thermal diffusivity for ten molecular liquids. In these liquids, the vibrational cooling rate of S_1 *trans*-stilbene, which represents microscopic solvation environments, is well accounted for by bulk thermal diffusivity.

In this article, we report on the observation of vibrational cooling process of S_1 *trans*-stilbene in seven ionic liquids. We compare the observed cooling rates with thermal diffusivities determined by the transient grating method. The results from two different experiments are explained if and only if we assume the presence of local structures in ionic liquids. We compare the observed cooling kinetics and a numerical model simulation with the diffusion equation of heat to estimate the size of local structure. A preliminary result for two ionic liquids has already been reported in a letter.[20]

II. EXPERIMENTAL SETUP

We use a picosecond time-resolved Raman spectrometer with two independently tunable light sources for the pump and probe pulses.[20,21] The output from a femtosecond mode-locked Ti:sapphire oscillator (Coherent, Vitesse, wavelength 800 nm, repetition rate 80 MHz, pulse duration 120 fs, average power 250 mW) was amplified by a Ti:sapphire regenerative-multipass amplifier (Quantronix Integra 2.5, wavelength 800 nm, repetition rate 1 kHz, pulse duration 2 ps, pulse energy 2.0 mJ). A half of the amplified pulse was separated and delivered to a β-barium borate crystal. The frequency-doubled output from the crystal pumped an optical parametric amplifier (OPA) (Light Conversion, TOPAS 4/400) to generate Raman probe pulses of 592 nm. The residual of the 800 nm amplified pulse pumped another OPA (Light Conversion, TOPAS 4/800), which generated the pump pulse of 296 nm or 325 nm. For determining precise Raman band positions in excess energy dependence measurements, we constructed a 4-f band pass filter that improved spectral resolution. The configuration of the 4-f band pass filter and its performance will be reported elsewhere.[22] Spectral and time resolution were set to 8 cm^{-1} and 4.0 ps, respectively, with the band pass filter. Wavelength of the pump pulse was set to 296 and 325 nm, corresponding to the excess energy of 2500 and 0 cm^{-1}, respectively.

The pump and probe pulses, traveling a common light path after a dichroic mirror, were focused onto the sample solution, which was held in a rotating quartz cell or was circulated through a dye laser jet nozzle. The pump and probe pulse energies at the sample point were 0.50 and 0.25 μJ, respectively. Rayleigh scattering and fluorescence in the ultraviolet region were eliminated by an optical narrow band-rejection filter (Kaiser Optical Systems, Notch filter) and an optical color filter. Scattered light was dispersed by a single imaging spectrograph (Horiba Jobin Yvon, Triax-320) and detected by a liquid-nitrogen cooled CCD detector (Princeton Instruments, Spec 10:400B/LN). Time resolution of this apparatus estimated by the rise time of S_n-S_1 absorption of *trans*-stilbene was 2.2 ps. The spectral resolution with a slit width of 100 μm was 13 cm^{-1}.

Sample of *trans*-stilbene was purchased from Wako Chemicals (special grade) and was recrystallized from ethanol. C_4mimTf_2N (1-butyl-3-methylimidazolium bis(trifluoromethylsulfonyl)amide, lot number 609041) was purchased from Kanto Chemical Co., Inc. $BmpyTf_2N$ (1-butyl-1-methylpyrrolidinium bis(trifluoromethylsulfonyl)amide) and C_4mimPF_6 (1-butyl-3-methylimidazolium hexafluorophosphate) were purchased from Fluka and used without further purification. C_2mimTf_2N (1-ethyl-3-methylimidazolium bis(trifluoromethylsulfonyl)amide), C_5mimTf_2N (1-pentyl-3-methylimidazolium bis(trifluoromethylsulfonyl)amide), C_6mimTf_2N (1-hexyl-3-methylimidazolium bis(trifluoromethylsulfonyl)amide), and C_8mimTf_2N (1-octyl-3-methylimidazolium bis(trifluoromethylsulfonyl)amide) were synthesized by previously reported method.[23] The ionic liquid samples were evacuated by a diffusion pump for 2 h or longer for removing water before Raman measurements. Concentration of *trans*-stilbene was 5.0×10^{-3} mol dm^{-3}.

The experimental setup for the TG method has been described in Ref. 24. As the photo-absorbing solute molecule, we used malachite green. The 532 nm second harmonic of a Nd:YAG laser (Spectra-physics GCR-170-10) was used as the excitation pulse. This excitation pulse was split by a beam splitter and crossed into a sample solution with a fixed angle. At the same time, a diode laser beam (780 nm) was brought into the sample solution with an angle which satisfied the Bragg condition. The diffracted probe beam (TG signal) was detected by a photomultiplier tube (Hamamatsu R928) and averaged by a digital oscilloscope (Tektronix TDS-5054).

III. RESULTS AND DISCUSSION

A. Vibrational cooling process and ultrafast solute-solvent energy transfer

Time-resolved Raman spectra of S_1 *trans*-stilbene were recorded at time delays of −20, −2, 0, 2, 3, 5, 7, 10, 15,

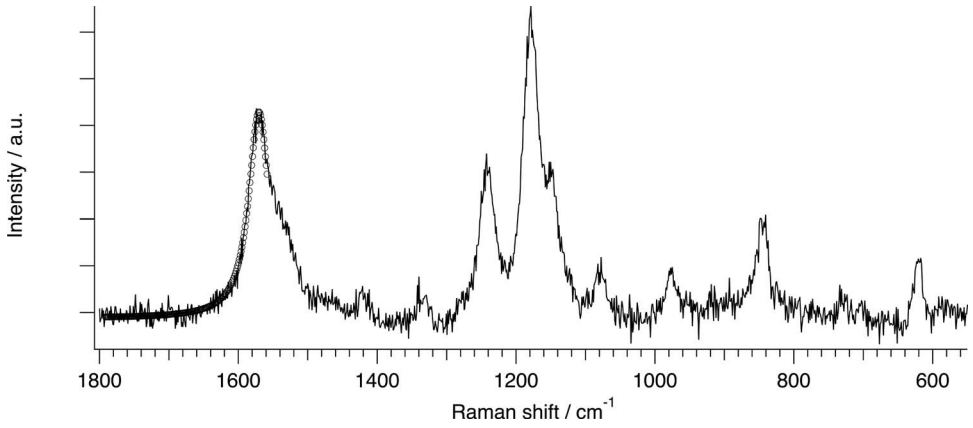

FIG. 1. Transient Raman spectrum of S_1 *trans*-stilbene in C_5mimTf_2N at 10 ps (solid line) and Lorentz function best fitted to the 1570-cm^{-1} band (open circle). Raman probe and pump wavelengths are 592 and 296 nm, respectively.

20, 30, 50, 70, and 100 ps. Transient Raman spectrum observed at each time delay agreed with the spectra measured in molecular solvents.[25–27] The transient Raman spectrum of S_1 *trans*-stilbene in C_5mimTf_2N at 10 ps is shown in Figure 1. Shot noise resulting from fluorescence was larger in ionic liquids than in molecular solvents. It was possible, however, to determine the exact peak position of the 1570-cm^{-1} Raman band, which corresponds to the central C=C stretch vibration of S_1 *trans*-stilbene. The position of this band is used as "picosecond Raman thermometer" as described in more details later. The observed 1570-cm^{-1} Raman band in ionic liquids is fitted well by a single Lorentz function, as was the case in molecular liquids. The uncertainty of fitted band position was 0.3 cm^{-1}.

Time dependence of the peak position of the 1570-cm^{-1} Raman band represents the vibrational cooling process of S_1 *trans*-stilbene after photoexcitation with an excess energy. The peak position determined from the fitting analysis is plotted against time delay in Figure 2(a). The peak position changes from 1567 to 1573 cm^{-1} as time delay increases. As already shown, the peak position of the 1570 cm^{-1} changes linearly with temperature and is used as a thermometer with a picosecond time resolution.[18] The time dependence shown in Figure 2(b) indicates that the cooling kinetics of S_1 *trans*-stilbene in C_5mimTf_2N is very similar to that observed in molecular liquids; this decay curve is well fitted by a single exponential function with a rate constant of 0.11 ps^{-1}. The single exponential function serves as a simple model function that characterizes the cooling kinetics with a single time constant.

B. Comparison of vibrational cooling rate with thermal diffusivity

We compare here the observed vibrational cooling rates with thermal diffusivities of ionic liquids measured by the transient grating method.[17] The observed vibrational cooling rates are plotted against thermal diffusivities in Figure 3, together with the corresponding results for molecular liquids. The vibrational cooling rates in molecular liquids show a good correlation with thermal diffusivities as reported earlier.[18] The observed cooling rate in ionic liquids, however, ranges from 0.082 to 0.12 ps^{-1} and are similar with those observed in molecular liquids, although thermal diffusivities of ionic liquids (5.4×10^{-8} to 7.5×10^{-8} m^2 s^{-1}) are obviously smaller than those of molecular liquids (8.0×10^{-8} to

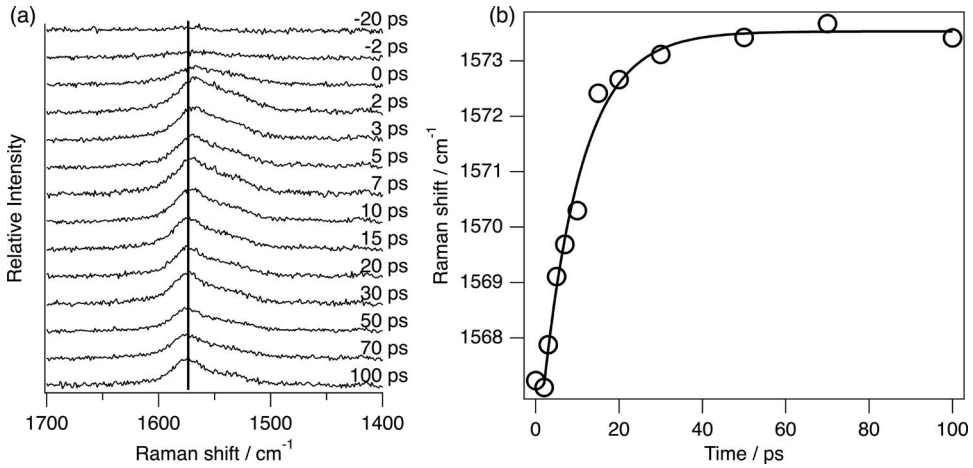

FIG. 2. Time-resolved Raman spectra of S_1 *trans*-stilbene in C_5mimTf_2N (a), and time dependence of the peak position of the 1570-cm^{-1} Raman band (b). Raman probe and pump wavelengths are 592 and 296 nm, respectively.

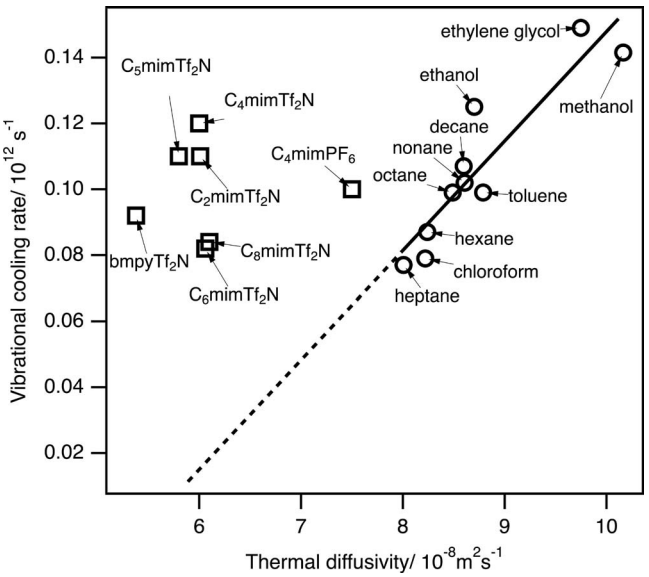

FIG. 3. Vibrational cooling rate vs thermal diffusivity plot for ionic and molecular liquids.

10×10^{-8} m^2 s^{-1}). The vibrational cooling rates show no clear correlation with thermal diffusivities in ionic liquids. It should be noted that the vibrational cooling rates in ionic liquids are similar with those in alkane solvents, suggesting that the *trans*-stilbene molecule is solvated selectively in alkane-rich environments in ionic liquids.

Thermal diffusivity κ is defined in the diffusion equation of heat as follows:

$$\frac{\partial \theta}{\partial t} = \frac{\lambda}{c\rho}\Delta\theta = \kappa\Delta\theta, \tag{1}$$

where θ is temperature, t is time, λ is thermal conductivity, c is specific heat, ρ is mass density, and Δ is the Laplacian ($\Delta = \partial^2/\partial x^2 + \partial^2/\partial y^2 + \partial^2/\partial z^2$). Thermal diffusivity κ represents the rate of temperature change caused by heat conduction, which is characterized by thermal conductivity λ, in a media. We are comparing here the vibrational cooling rate determined by "picosecond Raman thermometer" with thermal diffusivity in Eq. (1). For molecular liquids, we observed a good correlation between the two quantities. In ionic liquids, however, there is no obvious correlation observed between them.

The lack of correlation between the vibrational cooling rate and thermal diffusivity is well accounted for if we assume a non-uniform structure for ionic liquids. The vibrational cooling kinetics is controlled mainly by the solvent-solvent energy transfer process from molecules, or ions, in the first solvation shell toward the bulk. Thermal diffusivity, however, is measured for thermal conduction over a range of micrometers or longer. If there is a boundary between adjacent local structures where thermal energy transfer is decelerated, observed thermal diffusivity for bulk solvent will be reduced. The vibrational cooling rate reflects the energy transfer kinetics within microscopic solvation environments, while thermal diffusivity represents macroscopic heat conduction capability of bulk solvent.

In previous papers, we proposed that local structures, which preserve at least a part of the ordered structures of crystals, are present in ionic liquids. We also suggested that alkyl chains of cations form a domain structure in ionic liquids. These local structures, if they exist, make boundaries between adjacent domains. The rate of heat conduction over a boundary is expected to be much smaller than the heat transfer rate within a domain. The heat conduction rate over a boundary controls macroscopic thermal diffusion in ionic liquids and therefore macroscopic thermal diffusion is not a direct extension of microscopic thermal diffusion within a boundary. Thermal diffusivity measured for bulk solvent might well show a smaller value than what is expected from the energy transfer rate within microscopic solvation environments.

The vibrational cooling rate, which we observe from picosecond time-resolved Raman experiments, is determined by thermal diffusivity of solvation environments, or "local" thermal diffusivity. For molecular solvents with no boundary for thermal diffusion, local thermal diffusivity accords well with bulk thermal diffusivity. In ionic liquids, however, direct correlation is lost between local and bulk thermal diffusivities. In the following analysis, we estimate local thermal diffusivity in ionic liquids from the observed rate of vibrational cooling.

C. Numerical simulation of thermal diffusion in ionic liquids with local thermal diffusivity

We analyze the observed kinetics of the vibrational cooling process in ionic liquids with a simple numerical model. In our previous paper,[18] the vibrational cooling kinetics of S_1 *trans*-stilbene in chloroform was very well expressed with a solution of the diffusion equation of heat.[28,29] We therefore use the same equation for the following analysis of vibrational cooling kinetics:

$$\begin{aligned}\theta(x, y, z, t) - T_{r.t.} = (4\pi\kappa t)^{-3/2} \int_{-\infty}^{\infty}\int_{-\infty}^{\infty}\int_{-\infty}^{\infty} f(x', y', z') \\ \times \exp\{-[(x-x')^2 + (y-y')^2 \\ + (z-z')^2]/4\kappa t\} dx' dy' dz',\end{aligned} \tag{2}$$

where $\theta(x, y, z, t)$ is temperature at the position (x, y, z) at time t, $T_{r.t.}$ is room temperature, and $f(x, y, z)$ is the initial distribution of temperature change,

$$f(x, y, z) = \theta(x, y, z, 0) - T_{r.t.}. \tag{3}$$

It is assumed that the solute molecule and the nearest solvent molecules or ions are in thermal equilibrium immediately after photoexcitation. The initial distribution function $f(x, y, z)$ is then represented by a box function

$$f(x, y, z) = \begin{cases} T_\Delta & (|x| < a,\ |y| < b,\ |z| < c) \\ 0 & (\text{otherwise}) \end{cases}, \tag{4}$$

where T_Δ is the initial temperature change. By substituting $f(x, y, z)$ of Eq. (2) with Eq. (4), we obtain

$$\begin{aligned}&\theta(x, y, z, t) - T_{r.t.} \\ &= T_\Delta/8\{\mathrm{erf}((a-x)/(4\kappa t)^{1/2}) + \mathrm{erf}((a+x)/(4\kappa t)^{1/2})\}\end{aligned}$$

$$\times\{\mathrm{erf}((b-y)/(4\kappa t)^{1/2}) + \mathrm{erf}((b+y)/(4\kappa t)^{1/2})\}$$
$$\times\{\mathrm{erf}((c-z)/(4\kappa t)^{1/2}) + \mathrm{erf}((c+z)/(4\kappa t)^{1/2})\}, \quad (5)$$

where erf represents an error function defined as

$$\mathrm{erf}(x) = \frac{2}{\sqrt{\pi}} \int_{-\infty}^{x} \exp(-t^2)dt. \quad (6)$$

The dimensions of the initial heat distribution box are taken as $a = \alpha + r_0$, $b = \beta + r_0$, and $c = \gamma + r_0$, where α, β, and γ are the dimensions of the *trans*-stilbene molecule ($\alpha = 0.65$ nm, $\beta = 0.35$ nm, and $\gamma = 0.10$ nm) (Ref. 18) and r_0 represents the thickness of the solvent layer. Then temperature monitored at $(x, y, z) = (0, 0, 0)$ is given as

$$\theta(0,0,0,t) - T_{r.t.}$$
$$= T_\Delta \mathrm{erf}\{(\alpha + r_0)/(4\kappa t)^{1/2}\}\mathrm{erf}\{(\beta + r_0)/(4\kappa t)^{1/2}\}$$
$$\times \mathrm{erf}\{(\gamma + r_0)/(4\kappa t)^{1/2}\}. \quad (7)$$

We simulate the observed vibrational cooling kinetics using Eq. (7) with the initial temperature increase, T_Δ, and the thickness of the solvent layer, r_0, as fitting parameters.

Thermal diffusivity κ in Eq. (7) represents "local" thermal diffusivity. We estimate local thermal diffusivity from the vibrational cooling rate, by assuming the linear relation between the vibrational cooling rate and thermal diffusivity observed in molecular liquids (Fig. 3). For example, C_5mimTf_2N shows vibrational cooling rate constant of 0.11 ps^{-1}, which corresponds to "local" thermal diffusivity of 8.8×10^{-8} m^2 s^{-1}. The values of estimated local thermal diffusivity for the five ionic liquids are listed in Table I.

Vibrational cooling curves observed in the five ionic liquids, C_2mimTf_2N, C_4mimTf_2N, C_5mimTf_2N, C_6mimTf_2N, and C_8mimTf_2N, as well as in three molecular liquids, heptane, decane, and ethanol, have been successfully explained by Eq. (7). The result for C_5mimTf_2N is shown in Figure 4. The cooling kinetics is very well simulated with optimized parameters of $T_\Delta = 64$ K and $r_0 = 1.25$ nm. The simulation also reproduces very well the observed kinetics for the other four ionic liquids and the three molecular liquids. The T_Δ and r_0 values for the other solvents are listed in Table I. There are no large differences between the T_Δ and r_0 values in ionic liquids and molecular liquids. Solvation structure around S_1 *trans*-stilbene in the five ionic liquids is considered to be similar to that in molecular liquids.

TABLE I. Thickness of the solvent layer r_0, initial temperature increase T_Δ, "local" thermal diffusivity estimated from the numerical model simulation of thermal diffusion.

Solvent	Thickness of the nearest solvent layer (nm)	Initial temperature increase (K)	"Local" thermal diffusivity (10^8 m^2 s^{-1})
Heptane	1.26		...
Decane	1.39		...
Ethanol	1.11		...
C_2mimTf_2N	1.16	59	8.8
C_4mimTf_2N	1.17	74	8.8
C_5mimTf_2N	1.25	64	8.8
C_6mimTf_2N	1.17	71	8.1
C_8mimTf_2N	1.05	66	8.2

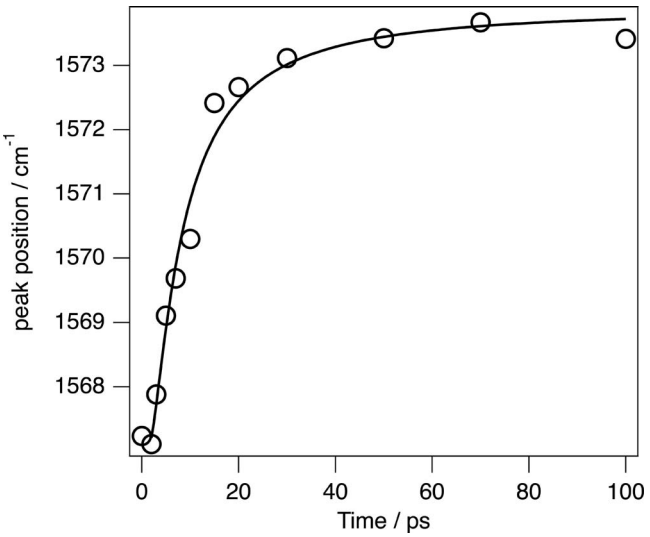

FIG. 4. Time dependence of the peak position of the 1570-cm^{-1} Raman band which represents the cooling kinetics (open circle) and simulated kinetics (solid curve) for C_5mimTf_2N.

D. Vibrational cooling kinetics with and without excess energy

Vibrational cooling kinetics of S_1 *trans*-stilbene with and without excess energy were examined for 0–200 ps. Figure 5 shows the temporal peak shifts of the 1570-cm^{-1} Raman band of S_1 *trans*-stilbene in C_2mimTf_2N with pump wavelengths of 296 nm (2500 cm^{-1} excess energy) and 325 nm (no excess energy). The peak shifts observed around the time origin, which have been attributed to strong electric field caused by

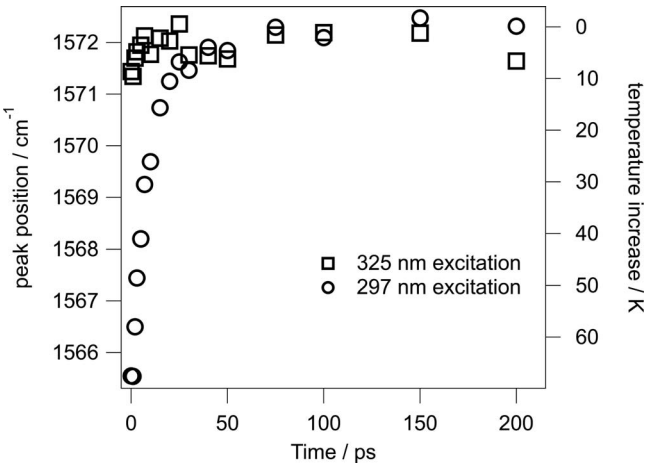

FIG. 5. Time dependence of the position of the 1570-cm^{-1} Raman band of S_1 *trans*-stilbene in C_2mimTf_2N for excitation wavelengths of 325 nm (square) and 296 nm (circle). Raman probe wavelength is 592 nm. The temperature increase estimated from the position of the 1570-cm^{-1} Raman band is indicated on the right ordinate.

an overlap of the probe and pump pulses,[30] are excluded from the following analysis. There is no large peak shift for 325 nm excitation, while a large shift corresponding to vibrational cooling is observed for 296 nm excitation. No temperature increase is expected for 325 nm excitation that carries no excess energy. The peak position stays constant showing that the temperature of S_1 *trans*-stilbene is equal to room temperature at all time delays. The temperature increase for 296 nm excitation estimated from the linear relationship between the peak position and temperature of S_1 *trans*-stilbene[25] is indicated on the right ordinate in Fig. 5. The agreement between the peak shifts with and without excess energy indicates that, even for 296 nm excitation, temperature recovers to the room temperature after 30 ps. The excess energy given to S_1 *trans*-stilbene upon photoexcitation fully dissipates to outer bulk solvent ions in a local structure with no detectable temperature increase.

From the observation that the excess energy dissipates completely within a local structure formed in C_2mimTf_2N, we are able to estimate the minimum volume of local structure. Slow heat transfer is expected at a boundary of local structure as we discuss for Fig. 3. If the volume of local structure is small enough, the excess energy remaining in a local structure causes a temperature increase. However, we did not observe such a temperature increase after 30 ps. The local structure in C_2mimTf_2N should have a volume large enough, for the excess energy of 2500 cm^{-1}, dissipates fully to make no detectable temperature increase.

E. Numerical simulation of thermal diffusion in local structure of ionic liquids

Here, we analyze the observed vibrational cooling curve of S_1 *trans*-stilbene in C_2mimTf_2N with pump wavelength of 296 nm (2500 cm^{-1} excess energy) in order to estimate the size of local structure. We use a new numerical model based on the same kinetic model as in Sec. III C. Thermal diffusion within a local structure is modeled with the heat dissipation from a heat source into a finite volume, which is represented by a cube with length L. We assume no heat flow at the boundary between local structures and that all excess energy from S_1 *trans*-stilbene stays within a local structure. This condition is modeled mathematically by assuming that heat flow is reflected back at the edge of the cube and is superposed on the original flow.[29] The result should reflect the nature of heat diffusion within the volume, although the energy flow across local structures would surely reduce the amount of heat within a local structure and therefore the estimated size of local structure here may be exaggerated.

If thermal diffusion occurs only in a cube with a length L, the solution of the diffusion equation gives the spatiotemporal profile of temperature $\theta(x, y, z, t)$ as[29]

$$\begin{aligned}\theta(x,y,z,t) - T_{r.t.} = {} & T_\Delta/8 \\ & \times \sum_{n=-\infty}^{\infty} \{\mathrm{erf}((a+x+nL)/(4\kappa t)^{1/2}) + \mathrm{erf}((a-x-nL)/(4\kappa t)^{1/2})\} \\ & \times \sum_{n=-\infty}^{\infty} \{\mathrm{erf}((b+y+nL)/(4\kappa t)^{1/2}) + \mathrm{erf}((b-y-nL)/(4\kappa t)^{1/2})\} \\ & \times \sum_{n=-\infty}^{\infty} \{\mathrm{erf}((c+z+nL)/(4\kappa t)^{1/2}) + \mathrm{erf}((c-z-nL)/(4\kappa t)^{1/2})\}. \end{aligned} \quad (8)$$

The temperature at the coordinate origin $(x, y, z) = (0, 0, 0)$ is therefore

$$\begin{aligned}\theta(0,0,0,t) - T_{r.t.} = {} & T_\Delta/8 \\ & \times \sum_{n=-\infty}^{\infty} \{\mathrm{erf}((a+nL)/(4\kappa t)^{1/2}) + \mathrm{erf}((a-nL)/(4\kappa t)^{1/2})\} \\ & \times \sum_{n=-\infty}^{\infty} \{\mathrm{erf}((b+nL)/(4\kappa t)^{1/2}) + \mathrm{erf}((b-nL)/(4\kappa t)^{1/2})\} \\ & \times \sum_{n=-\infty}^{\infty} \{\mathrm{erf}((c+nL)/(4\kappa t)^{1/2}) + \mathrm{erf}((c-nL)/(4\kappa t)^{1/2})\}. \end{aligned} \quad (9)$$

As the sum of series for each coordinate converges rapidly with a small number of terms, it is calculated from n = −10 to 10 in the present analysis.

We compare the observed cooling kinetics with the numerical simulation with Eq. (9). All the parameters in Eq. (9) except for L are fixed to the same value as obtained in

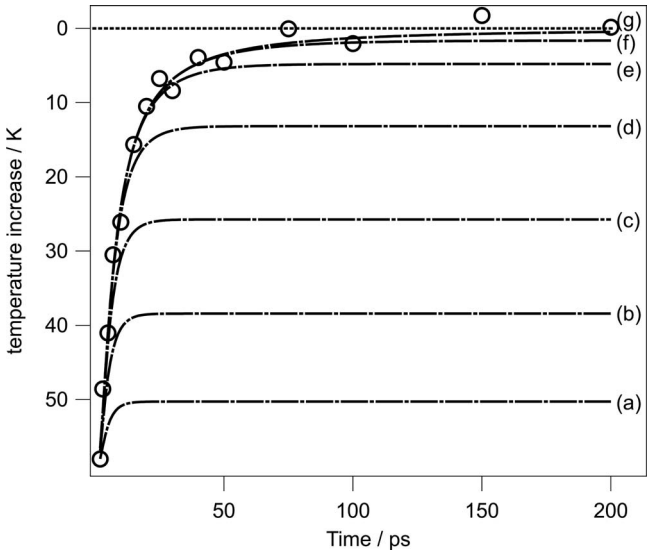

FIG. 6. Time dependence of the temperature increase of S_1 *trans*-stilbene simulated with the length L of 3.2 (a), 3.5 (b), 4.0 (c), 5.0 (d), 7.0 (e), 10 (f), and 50 nm (g). The observed values are shown with open circles. The dotted line indicates the peak position for room temperature. The initial temperature rise T_Δ is 59 K.

Sec. III C. L is the only adjustable parameter. We limit the time range of simulation to 2–200 ps in order to remove the influence of the artifacts observed in early time delays. The results for L values in the range of 3.2–50 nm are shown in Figure 6. It is obvious that the simulated cooling kinetics with an L value of 10 nm or larger reproduces the observed cooling kinetics very well, showing complete recovery to room temperature after 30 ps. However, the simulated kinetics stops cooling before reaching room temperature if the L value is 7.0 nm or smaller. For smaller L values, temperature does not cool down to room temperature because heat is not fully dissipated, as we have discussed already in Sec. III D. The comparison between the observed and simulated cooling kinetics shows that the diameter of local structure is most likely to be larger than 10 nm.

F. Local structure in ionic liquids

It has been shown that some of the solvation environments detected by ultrafast spectroscopic methods are not directly correlated with macroscopic properties of bulk ionic liquids. It has been known well that the photoisomerization rate of *trans*-stilbene correlates well with viscosity of bulk solvent in molecular liquids. The photoisomerization rate observed in C_4mim[PF_6], however, was larger by more than an order of magnitude than the rate estimated from its viscosity if the relationship between the isomerization rate and viscosity for molecular liquids was assumed.[31] The rotational diffusion time of a solute molecule often has a linear correlation with solvent viscosity, as indicated by the Debye-Stokes-Einstein theory. In ionic liquids, however, the rotational diffusion time of 2-aminoquiline did not correlate with its viscosity.[32] Photo-thermalization rate of malachite green did not show a linear relationship with the solvent viscosity of ionic liquids.[33]

The lack of correlation between solvation environments and macroscopic properties in ionic liquids is consistent with the presence of local structures discussed by several groups.[1–4,8–11,34] Because of the boundary that originates from local structures, microscopic solvation environments cannot be directly extrapolated to macroscopic properties. Considering the fact that ionic liquids are all transparent, the size of local structure must be much smaller than the wavelength of visible light. This fact imposes the upper limit of 100 nm. Combined with the present estimation of the lower limit, 10 nm, an order of magnitude estimate of the size of local structure is obtained as 10 nm $< L <$ 100 nm, where L stands for the length or the diameter of local structure.

IV. CONCLUSIONS

The vibrational cooling rate was measured in ionic liquids with the peak position of the 1570-cm^{-1} Raman band of S_1 *trans*-stilbene, or "picosecond Raman thermometer". Unlike in molecular liquids, the vibrational cooling rate in ionic liquids showed no correlation with bulk thermal diffusivities. The vibrational cooling rate reflects solvent-solvent energy transfer rate within a microscopic region around the solute. The presence of local structure, which has been proposed by several researchers, explains well this lack of correlation. Macroscopic thermal diffusion is controlled by heat conduction across the boundaries of local structures, while microscopic thermal diffusion is controlled by energy transfer within a local structure. We should note that microscopic properties of ionic liquids are not well represented by bulk solvent properties like polarity and viscosity.

It is necessary to characterize microscopic environments in ionic liquids with "local" properties that are defined within a local structure. The idea of local property, such as local thermal diffusivity we discuss in this article, will be important to examine in details the microscopic environments in inhomogeneous media, which includes micelles,[35] vesicles, or cell membranes as well as ionic liquids.

Observation of the vibrational cooling process and its dependence on the amount of excess energy is crucial for estimating the size of local structure. A model simulation for this observation allows us to estimate the lower limit of the size of local structure in C_2mimTf_2N as 10 nm.

ACKNOWLEDGMENTS

This work is supported by grant-in-aid for Creative Scientific Research (Grant No.11NP0101) from Japan Society for the Promotion of Science (JSPS), and by grant-in-aid for Scientific Research on Priority Areas (Area 452, Grant No. 17073003) and Global COE Program (The University of Tokyo Global COE Chemistry Innovation through Cooperation of Science and Engineering) from the Ministry of Education, Culture, Sports, Science and Technology (MEXT) of the Japanese Government.

[1] K. Iwata, H. Okajima, S. Saha, and H. Hamaguchi, Acc. Chem. Res. **40**, 1174 (2007).
[2] A. Triolo, O. Russina, H.-J. Bleif, and E. D. Cola, J. Phys. Chem. B **111**, 4641 (2007).

[3]S. Saha, S. Hayashi, A. Kobayashi, and H. Hamaguchi, Chem. Lett. **32**, 740 (2003).
[4]H. Katayanagi, S. Hayashi, H. Hamaguchi, and K. Nishikawa, Chem. Phys. Lett. **392**, 460 (2004).
[5]J. Dupont, J. Braz. Chem. Soc. **15**, 341 (2004).
[6]A. Triolo, O. Russina, C. Hardacre, M. Nieuwenhuyzen, M. A. Gonzalez, and H. Grimm, J. Phys. Chem. B **109**, 22061 (2005).
[7]Y. Inamura, O. Yamamuro, S. Hayashi, and H. Hamaguchi, Physica B **385–386**, 732 (2006).
[8]U. Schroder, J. Wadhawan, R. G. Compton, F. Marken, P. A. Z. Suarez, C. S. Consorti, R. F. de Souza, and J. Dupont, New J. Chem. **24**, 1009 (2000).
[9]H. Tokuda, K. Hayamizu, K. Ishii, M. A. B. H. Susan, and M. Watanabe, J. Phys. Chem. B **108**, 16593 (2004).
[10]M. Fukuda, M. Terazima, and Y. Kimura, J. Chem. Phys. **128**, 114508 (2008).
[11]Y. Wang and G. A. Voth, J. Am. Chem. Soc. **127**, 12192 (2005).
[12]J. N. A. C. Lopes and A. A. H. Padua, J. Phys. Chem. B **110**, 3330 (2006).
[13]M. G. D. Popolo and G. A. Voth, J. Phys. Chem. B **108**, 1744 (2004).
[14]Y. Wang and G. A. Voth, J. Phys. Chem. B **110**, 18601 (2005).
[15]Z. Hu and C. J. Margulis, Proc. Natl. Acad. Sci. U.S.A. **103**, 831 (2006).
[16]R. Ozawa and H. Hamaguchi, Chem. Lett. **30**, 736 (2001).
[17]C. Frez, G. J. Diebold, C. D. Tran, and S. Yu, J. Chem. Eng. Data **51**, 1250 (2006).
[18]K. Iwata and H. Hamaguchi, J. Phys. Chem. A **101**, 632 (1997).
[19]R. E. Hester, P. Matousek, J. N. Moore, A. W. Parker, W. T. Toner, and M. Towrie, Chem. Phys. Lett. **208**, 471 (1993).
[20]K. Iwata, K. Yoshida, Y. Takada, and H. Hamaguchi, Chem. Lett. **36**, 504 (2007).
[21]K. Iwata, J. Raman Spectrosc. **39**, 1512 (2008).
[22]K. Yoshida, Ph.D. thesis, The University of Tokyo, 2012.
[23]P. Bonhôte, A.-P. Dias, N. Papageorgiou, K. Kalyanasundaram, and M. Grätzel, Inorg. Chem. **35**, 1168 (1996).
[24]Y. Nishiyama, M. Fukuda, M. Terazima, and Y. Kimura, J. Chem. Phys. **128**, 164514 (2008).
[25]H. Hamaguchi and K. Iwata, Bull. Chem. Soc. Jpn. **75**, 883 (2002).
[26]H. Hamaguchi, C. Kato, and M. Tasumi, Chem. Phys. Lett. **100**, 3 (1983).
[27]T. L. Gustafson, D. M. Roberts, and D. A. Chemoff, J. Chem. Phys. **79**, 1559 (1983).
[28]H. S. Carslaw and J. C. Jaeger, *Conduction of Heat in Solids*, 2nd ed. (Oxford University Press, Oxford, 1959).
[29]J. Crank, *The Mathematics of Diffusion*, 2nd ed. (Oxford University Press, Oxford, 1975).
[30]K. Iwata, Bull. Chem. Soc. Jpn. **75**, 1075 (2002).
[31]R. Ozawa and H. Hamaguchi, Chem. Lett. **30**, 736 (2001).
[32]K. Iwata, M. Kakita, and H. Hamaguchi, J. Phys. Chem. B **111**, 4914 (2007).
[33]M. Fukuda, O. Kajimoto, M. Terazima, and Y. Kimura, J. Mol. Liq. **134**, 49 (2007).
[34]H. Hamaguchi and R. Ozawa, Adv. Chem. Phys. **131**, 85 (2005).
[35]K. Iwata and H. Hamaguchi, J. Raman Spectrosc. **29**, 915 (1998).